Preparation and performance of ultra-thin surface coated pervaporation membranes for seawater purification

F. U. Nigiz

ABSTRACT

In this study, ultra-thin poly(ether-block-amide, PEBA)-coated poly(vinyl alcohol, PVA) composite membranes were prepared and assessed for the removal of lead, zinc, lithium, arsenic, and copper from seawater. Effects of the coating numbers and temperature on flux and ion rejection were evaluated. The number of coating processes increased the thicknesses of the membranes. The ion rejection and water flux decreased with the increasing coating process. Dissolved ions were retained with a rejection of >99.5%. The highest rejections of 99.99% and 99.98% were obtained for sodium and magnesium ions. The coated PVA membranes showed a superior heavy-metal removal greater than 88%. The highest rejection improvements were obtained for zinc (Zn), lithium (Li), and copper (Cu) metals. The zinc, copper, and lithium rejections increased from 89.1%, 88.3%, and 85.1% to 95.3%, 98.46% and 94.4% due to the PEBA coating process, respectively. The influence of PVA thickness on the flux and rejection was also investigated. Increasing the thickness of PVA decreased the flux. The highest flux of 2.34 kg/m^2.h was obtained with the membrane having a thickness of 90 μm.

Key words | desalination, PEBA coated PVA, pervaporation

F. U. Nigiz
Department of Chemical Engineering,
University of Kocaeli,
41380 Kocaeli,
Turkey
E-mail: *filiz.ugurr@gmail.com*

INTRODUCTION

Membrane separation technologies have an important role in water purification. There are many membrane types characterized according to structural–chemical properties. Porous-type membranes are used for filtration (micro-ultra-nanofiltration) application (Le & Nunes 2016). Non-porous-type membranes are used for gas separation and pervaporation. While hydrophobic membranes are preferred for membrane distillation, hydrophilic membranes are used for pervaporative separation (Baker 2004; Nunes & Peinemann 2001, 2010). Each membrane type exhibits unique properties depending on its purpose in use. While porous structure and pore size are important for the filtration-type membrane that is maintained by the size exclusion phenomenon, the affinity of the membrane to the selected component is important for the non-porous membrane that is driven by the solution-diffusion mechanism (Wijmans & Baker 1995; Shao & Huang 2007; Ulbricht 2006). The water purification performance of a membrane depends on the flux, selectivity, separation factor, ion rejection, membrane durability, membrane stability, number of usage cycles without performance loss, etc. (Baker 2004; Nunes & Peinemann 2001, 2010). Therefore, the selection of the membrane material and module becomes a crucial factor for an efficient separation process.

Membrane-based desalination methods are based on the selective permeation of water through a semi-permeable membrane. Reverse osmosis (RO), forward osmosis (FO), electrodialysis (ED), and nanofiltration (NF) are well-known and commercialized desalination techniques (Nunes & Peinemann 2010; Gude 2018). Membrane distillation (MD) is another emerging membrane process (Goh *et al.* 2016). Among these, RO is well established and used

doi: 10.2166/ws.2019.053

commercially for seawater desalination. Non-porous or nano-porous membranes are used in RO. Different membrane materials (polymeric, inorganic or composite) can be used in RO (Greenlee *et al.* 2009; Lee *et al.* 2011)). The drawback of RO for desalination is the higher transmembrane pressure demand and the higher electrical energy consumption (Mazlan *et al.* 2016; Gude 2018). Moreover, rejection of some ions, such as boron, chloride, and bromide, can be low in a single-stage RO system.

Recently, significant investigations have been made in pervaporation (PV) seawater desalination (Gao 2016; Liu *et al.* 2018; Wu *et al.* 2018). The same as in RO, non-porous membranes are used for pervaporative desalination. In this process, the separation phenomenon is characterized by the solution-diffusion model. This model is basically based on the dissolution of the target component on the membrane's surface, diffusion across the membrane and desorption to the downstream side (Mulder 1996; Nunes & Peinemann 2001; Baker 2004). The transition of the target component occurs among the molecular spaces of the membrane. In the PV process, the driving force is chemical potential, which is created by the vacuum or inert purge gas pressure on the permeate side. Therefore, the electric energy consumption for PV is lower compared with RO. Because of the mild operating parameters (application at low temperature and atmospheric pressure), PV is defined as an energy saving, economical and clean technique. The separation mechanism through inorganic membranes or inorganic material incorporating polymeric pervaporative membranes can also be explained by size exclusion, charge exclusion, water permeation and surface evaporation phenomena (Cho *et al.* 2011; Wang *et al.* 2016). The free volume of the polymeric material is effective for pervaporative separation performance. The mobility of the adsorbed ions on the membrane, surface hydrophilicity–hydrophobicity of the membrane, physicochemical properties of the membrane, concentration of seawater and many other properties of seawater are effective for separation performance (Gude 2018; Thomas *et al.* 2018).

The concentration of the constituent in saline water, operating temperature, quantitative amount of the pressure difference between sides of the membrane, and condensation efficiency are the main factors to determine desalination performance (Gao 2016; Gude 2018). Besides the operating conditions, structural properties of the membrane play an important role in effective purification. Polymeric membranes have been frequently used due to their low-cost production route and ease of modification capability (Gao 2016). During pervaporation, water transition occurs through the intermolecular chains of the polymeric material. However, the high swelling and plasticization tendency of the polymeric structure may cause instability during the lengthy desalination period. According to the structural properties and thermal status of the polymer, polymeric materials are classified into two main groups: rubbery and glassy (Robeson *et al.* 2015; So *et al.* 2015). Mostly, water-selective membranes are fabricated from glassy polymers. The membrane synthesized from a glassy polymer shows less chain mobility, which determines the permeability of the target component. However, glassy polymers are brittle and show a surface defect tendency due to the higher glass transition temperature compared with the rubbery polymer. Therefore, some modifications are needed to keep stable the membrane's performance.

In this study, non-porous ultra-thin surface coated polyvinyl alcohol (PVA) membrane was prepared to purify water from heavy metals and other contaminants. Polyvinyl alcohol is a kind of hydrophilic polymer which is frequently used for selective water separation. However, PVA has a high water uptake capacity and swelling tendency. Hence, the stability and durability of the PVA-based membrane need to be improved by blending, cross-linking, inorganic material incorporation or other modification methods. In the literature, there are several studies on the use of a PVA membrane for desalination application. Xie *et al.* (2011) prepared a silica–PVA membrane for pervaporative desalination purposes and they reported that they found a NaCl rejection of 99.5%. Xue *et al.* (2019) also used a PVA membrane for NaCl–water separation by using a chemical cross-linking method to improve the PVA membrane. They also found a NaCl rejection of 99.5%. Zhang *et al.* (2017) fabricated a thin film membrane on a porous support and experimented for desalination of NaCl–water solution. They found the NaCl rejection to be 99.8%. In the literature, researchers have mostly focused on the separation performance of synthetic saline water using PVA-based membranes. Seawater not only contains high concentrations of dissolved salt ions but also consists of lots of minerals, heavy metals,

and ions which should be purified. Therefore, this study focused on heavy metal and ion rejection along with salt rejection. PVA was selected as the main membrane material. In order to prevent the excess swelling and to improve ion rejection, the PVA membrane was covered with a thin polyether block amide (PEBA) polymer in this study. PEBA is a copolymer that consists of hard amide and soft ethylene segments. Although PEBA polymer has a hydrophobic nature, it has been successfully prepared and used as a membrane. It exhibits superior purification performance. Membrane defects caused by water swelling have not been observed for PEBA membranes (Nigiz 2018). A few studies have reported the desalination performance of PEBA membranes. Marian *et al.* (2017) prepared and used a composite PEBA-based membrane for desalination of seawater. They obtained 99.9% rejection with 4.93 kg/m^2 h of flux. Wu *et al.* (2018) also prepared a PEBA-based pervaporation membrane and achieved 99.9% rejection. Compared with PVA, the flux values of PEBA are low and rejection values are high. Therefore, in the present study, PVA was covered with ultra-thin PEBA polymer to enhance rejection by eliminating the flux decline.

MATERIALS AND METHODS

Membrane preparation

PVA (MW, 125,000 g/mol) was firstly dissolved in deionized water and stirred for 4 hours at a temperature above 85 °C until a homogeneous polymer–water solution was obtained. The membrane solution was cast onto a glass surface and dried for 24 hours in an oven at 60 °C. The pristine PVA membrane was obtained as a flat sheet. Separately, 5 wt% of PEBA (Pebax2533)–ethanol solution was prepared. The pristine PVA membrane was coated with the prepared PEBA–ethanol solution by means of a dip coater at 40 °C, with a coating speed of 2 mm/s. Membranes were titled according to the numbers of the dip-coating (DC) runs. The numbers after the DC represented the number of the coating process. While DC-0 represented the pristine PVA membrane without coating, DC-1, DC-3, DC-5, and DC-7 represented the PVA membrane coated for one time, three, five and seven times, respectively. After each coating procedure, the membrane was allowed to dry for 20 minutes.

Membrane characterization

Morphological structures of the one-time and seven-times coated PVA membranes were characterized using a low-vacuum-type scanning electron microscope (SEM)(Jeol JSM-6510 with a detector of Oxford Instruments Inca EDS). The cross-section morphological analyses of membranes were done by fracturing in liquid nitrogen. Prior to analyzing, membranes were covered by platinum in order to provide a conductive effect and to avoid a charging effect in the membrane. A sputter coater was used for platinum covering and the thickness of the thin film platinum layer was approximately 20 nm. The analysis was operated at 10 kV with high magnifications of 7,000 and 20,000. The focal length of the lens was 15 mm.

Ion removal

Separation experiments were conducted in a pervaporation system that has been previously explained in the literature (Nigiz 2018). The system consists of a membrane cell, a vacuum pump, and cold traps. The volume capacity of the membrane cell was 250 ml. The effective separation area of the membrane was 19.6 cm^2. Seawater was fed onto the membrane cell and kept on the upstream side of the membrane during the separation. A mechanical stirrer was provided and seawater was continuously stirred with a stirring rate of 500 rpm to prevent mass-transfer limitations. During the experiments, the pressure of the feed side (upstream side of the membrane) was at atmospheric pressure and the permeate side was kept at 10 mbar pressure to create a driving force across the membrane. Desalination experiments were repeated three times and the average results are given with the standard deviation in the results. The separation performance of the experiment was evaluated in terms of flux and rejection. Water flux (F) (kg/m^2.h) and ion rejection (R) (%) were calculated using Equations (1) and (2), respectively:

$$F = \frac{W_p}{A.t} \quad (1)$$

$$R = \left(\frac{C_f - C_p}{C_f}\right) * 100 \quad (2)$$

where W_p is the weight of permeate (kg), A is the effective membrane area (m^2), t is the experiment period (h), C_f is the concentration of ions in the feed solution, and C_p is the concentration of ions in the permeate solution.

In order to determine the total conductance of the solutions, a Mettler Toledo, Seven Compact Device was used with a measurement accuracy of ±2 µS/cm. Concentrations of the other minerals and ions in the permeate solution were determined by means of a Perkin Elmer Elan DRC-e ICP-MS. The inductively coupled plasma mass spectrometry (ICP-MS) analysis details are given in Table 1.

RESULTS AND DISCUSSION

The polymer–polymer compatibility and the thickness of the membrane surface verified by the coating run were investigated using scanning electron microscopy (SEM).

Table 1 | ICP-MS operating parameters

(a) Instrumental parameters	
RF power	1,300 watts
Argon gas flow (L/min)	
• Plasma	15
• Auxiliary	1.2
• Nebulizer	0.98
Peristaltic pump flow (mL/min)	20
Sample uptake rate	~1
Skimmer cone	Pt (1.1 aperture diameter in mm)
Sampling cone	Pt (0.9 aperture diameter in mm)
(b) Data acquisition parameters	
Measurement mode	Standard, scan mode: peak hopping and DRC (dynamic reaction cell mode) for P, S and As using ultrapure oxygen as reaction gas 20 ppb Rh and Re internal standard
Number of measurements per peak	50
Mass range (m/z)	5–270 amu
Integration time	1,000 ms
Number of repetitions	3
Time per sample measurement	3 min 38 s (including 35 s sample flush)
Rinse time (s)	45 (plus ~ 15 s read delay)

Figure 1 shows the SEM results of membranes coated one time and seven times. The micrographs indicate that two different materials exhibited perfect interfacial compatibility. There was no interfacial gap between the surfaces of the structures. While the coating thickness of the single-coated membrane was about 0.26 µm, the thickness of the seven-times-coated PEBA layer was about 1.25 µm. The coating thickness almost linearly increased with the number of coating processes. The thickness of the PVA membrane was 220 µm.

In Figure 2, the water flux and total salt rejection results are shown as a function of the number of dip-coating processes. The dip-coating procedure was applied several times to the pristine PVA having an average thickness of 220 µm. Figure 2(a) shows the flux results. Increasing coating numbers decreased the water flux. There could be two possible reasons for the reduction of the water flux depending on the surface coating. One of the reasons should be related to Fick's law (Baker 2004), which explains the flux decrement with increasing membrane thickness. The other reason for the flux decrement could be related to the change in the surface roughness and wettability, which directly affected the surface affinity of the membrane to water. It is known that PEBA has a hydrophobic nature. In the present study, the PEBA coating could cause a decline in flux owing to the decrease in hydrophilicity of the membrane surface. Considering that the thickness of the coating on the surface was very thin compared with the total membrane thickness, reduction of the flux was more related to the decreasing surface wettability of the membrane.

Another observation obtained from Figure 2(a) is the effect of temperature on flux values. The highest flux was obtained in the pristine PVA membrane and the flux was also enhanced with the increasing temperature. Due to the increasing driving force resulting in increasing vapor pressure, water passage through the membrane was enhanced (Baker 2004). Concentrations of dissolved salt ions such as sodium, potassium, and calcium are higher than those of other ions and heavy metals in seawater. The PVA polymer exhibited superior performance towards the total dissolved solids. Contrary to flux values, increasing the coating process enhanced the total rejection slightly (Figure 2(b)). Generally, flux and rejection exhibit a trade-off

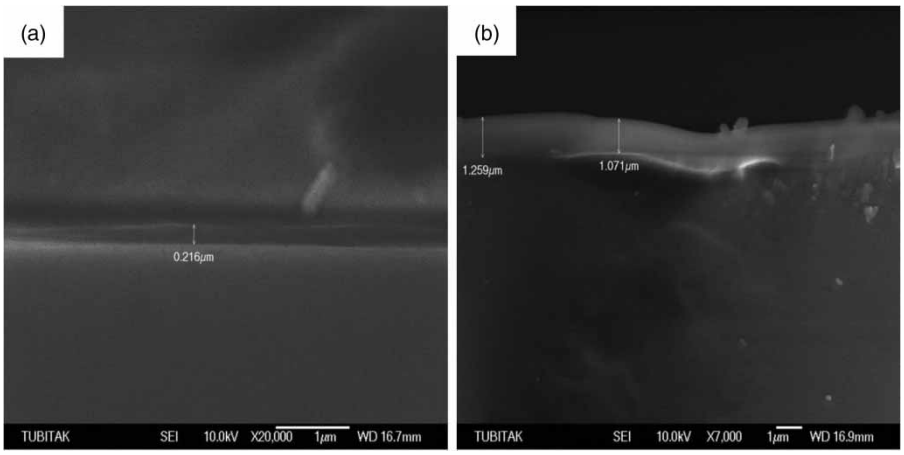

Figure 1 | SEM micrographs of (a) one-time and (b) seven-times PEBA-coated PVA membranes.

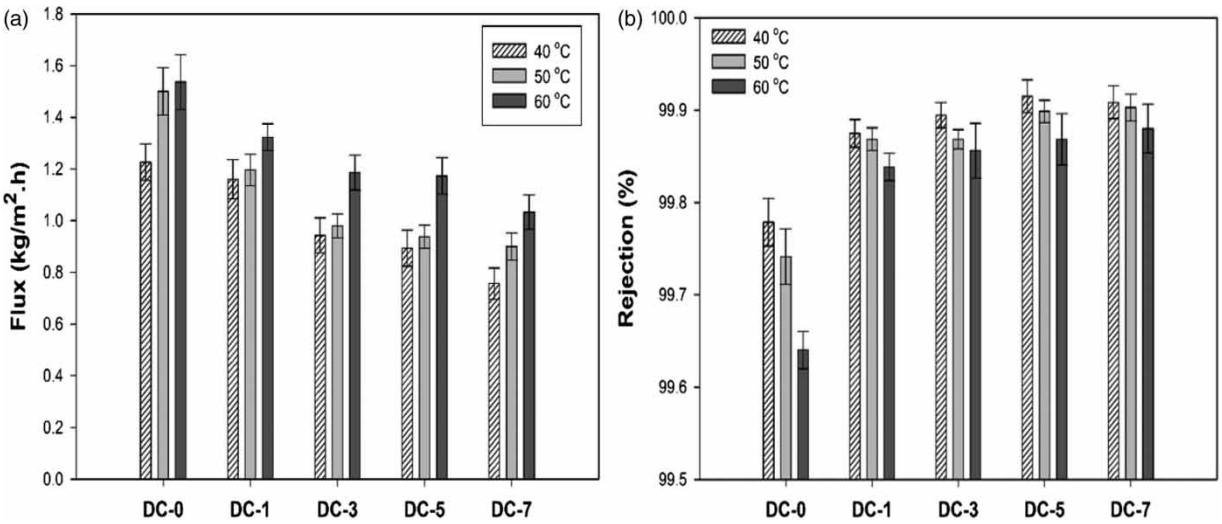

Figure 2 | Effect of dip-coating numbers on water flux and total salt rejection factor at constant temperature.

trend depending on the increasing temperature of the desalination process. Nevertheless, when results were carefully addressed, it was seen that the increase in rejection results depending on the coating run was not very significant. Greater than 99.5% rejection values were obtained in all experiments.

Figure 2(b) also shows the effect of temperature on rejection values. While the pristine PVA membrane was remarkably affected by the temperature increment, use of the PEBA-coated PVA membrane prevented the rejection decrement. In other words, the increasing temperature did not affect rejection values significantly. This result was attributed to the structural properties of the membrane. PVA is a glassy polymer and the glass transition temperature (T_g) of the PVA ranges from 50 °C to 80 °C (Xu *et al.* 2001; Magalhães *et al.* 2013). As the operating temperature approaches the glass transition temperature, the chain mobility of PVA polymer accelerates and the free volume of the intramolecular chain enlarges. Consequently, rejection values can decrease. It is known that the separation mechanism through non-porous polymeric membranes is directly related to the number of the free volume and the size of chain spaces of the polymer molecules (Wang *et al.* 2016). In this study, the PEBA-coating procedure might restrict the structural changes of the PVA membrane; consequently, the rejection decline was limited as illustrated in

Figure 2(b). In fact, using one layer already made improvements to salt rejection, with relatively small reduction in flux. On this basis, using one or two layers would be sufficient. It is difficult to increase the rate at very high rejections, hence the results are remarkable.

Figure 3 shows the influence of PVA thickness on water flux and total salt rejection when the number of coating processes was one. The figure indicates that the increasing membrane thickness caused a remarkable decrease in flux values and a slight increase in rejection values. As the membrane thickness increased from 90 µm to 220 µm, the water flux decreased from 2.34 kg/m^2.h to 1.16 kg/m^2.h. Pervaporation is a concentration-driven process; hence, the increasing transport thickness decreases the flux according to Fick's law. With the increasing membrane thickness, the thickness of the rigid dry layer on permeate size increases and the selective property of the membrane is enhanced. In the present study, the increase in the rejection was very slight (from 99.84% to 99.88%) compared with the decrease in the flux. Therefore, it would be better to use a thinner membrane for pervaporative desalination.

Figure 4 shows the heavy-metal rejection results of the non-coated PVA and PEBA-coated PVA membranes. Results were obtained from ICP-MS analysis. In Figure 4, the rejection results of several heavy metals including zinc (Zn), lithium (Li), copper (Cu), arsenic (As), lead (Pb) are included. As a result, it was found that the PVA-coating process substantially improved the Zn, Li, and Cu ion rejection capacity of the membrane.

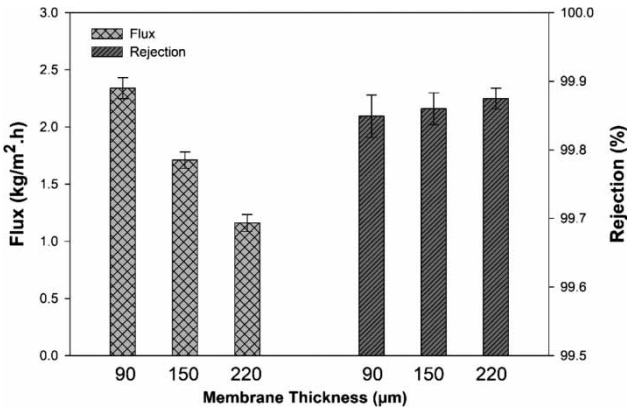

Figure 3 | Effect of membrane thickness on flux and rejection.

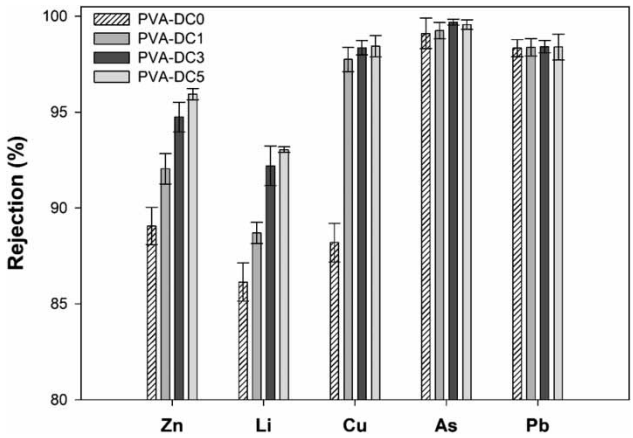

Figure 4 | Rejection of heavy metals.

CONCLUSIONS

In this study, ultra-thin PEBA-coated PVA composite membrane was prepared and used for removal of dissolved salt ions and heavy metals (lead, zinc, lithium, arsenic, copper) from seawater. Effects of coating numbers, temperature, and PVA thickness on water flux and ion rejection were investigated and results were evaluated. The main findings are summarized as follows:

- Increasing surface thickness decreased the flux and increased the rejection of ions.
- Greater than 99% of total ion rejections were achieved by using all membrane types.
- The highest rejections of 99.99% and 99.98% were obtained for sodium and magnesium ions.
- The zinc, copper, and lithium rejections increased from 89.1%, 88.3%, and 85.1% to 95.3%, 98.46% and 94.4% due to the PEBA-coating process, respectively.
- The highest flux of 2.34 kg/m^2.h was obtained with the PVA layer having a thickness of 90 µm.
- Coated PVA membranes showed superior heavy metal removal greater than 88%. The highest rejection improvements were obtained for Zn, Li, Cu metals.

Overall, PEBA-coated PVA membranes were effective in removing dissolved ions and heavy metals from seawater. Furthermore, the membranes exhibited superior rejection and proved their performance for use in other applications such as wastewater treatment.

ACKNOWLEDGEMENTS

The author would like to thank colleagues at ICP-Laboratory Kocaeli University for their assistance of ion analyzing. This study was supported by Kocaeli University Scientific Research Projects Coordination Unit (Grant Number: 2017/009).

REFERENCES

Baker, R. W. 2004 *Membrane Technology and Applications*, 2nd edn. J. Wiley, Chichester, UK.

Cho, C. H., Oh, K. Y., Kim, S. K., Yeo, J. G. & Sharma, P. 2011 Pervaporative seawater desalination using NaA zeolite membrane: mechanisms of high water flux and high salt rejection. *Journal of Membrane Science* **371** (1–2), 226–238.

Gao, A. 2016 *Desalination of High-Salinity Water by Membranes*. Master's thesis, University of Waterloo, Waterloo, Ontario, Canada.

Goh, P. S., Matsuura, T., Ismail, A. F. & Hilal, N. 2016 Recent trends in membranes and membrane processes for desalination. *Desalination* **391**, 43–60.

Greenlee, L. F., Lawler, D. F., Freeman, B. D., Marrot, B. & Moulin, P. 2009 Reverse osmosis desalination: water sources, technology, and today's challenges. *Water Research* **43** (9), 2317–2348.

Gude, V. G. 2018 *Emerging Technologies for Sustainable Desalination Handbook*. Butterworth-Heinemann, Cambridge, MA, USA.

Le, N. L. & Nunes, S. P. 2016 Materials and membrane technologies for water and energy sustainability. *Sustainable Materials and Technologies* **7**, 1–28.

Lee, K. P., Arnot, T. C. & Mattia, D. 2011 A review of reverse osmosis membrane materials for desalination – development to date and future potential. *Journal of Membrane Science* **370** (1–2), 1–22.

Liu, G., Shen, J., Liu, Q., Liu, G., Xiong, J., Yang, J. & Jin, W. 2018 Ultrathin two-dimensional MXene membrane for pervaporation desalination. *Journal of Membrane Science* **548**, 548–558.

Magalhães, M. S., Toledo Filho, R. D. & Moraes Rego Fairbairn, E. 2013 Durability under thermal loads of polyvinyl alcohol fibers. *Revista Matéria* **18**, 1587–1595.

Marian, S. A., Asghari, M. & Amini, Z. 2017 Desalination of Kashan City's water using PEBA-based nanocomposite membranes via pervaporation. *J. Water Environ. Nanotechnol.* **2** (2), 96–102.

Mazlan, N. M., Peshev, D. & Livingston, A. G. 2016 Energy consumption for desalination – a comparison of forward osmosis with reverse osmosis, and the potential for perfect membranes. *Desalination* **377**, 138–151.

Mulder, M. 1996 *Basic Principles of Membrane Technology*, 2nd edn. Kluwer, Dordrecht, The Netherlands.

Nigiz, F. U. 2018 Preparation of high-performance graphene nanoplate incorporated polyether block amide membrane and application for seawater desalination. *Desalination* **433**, 164–171.

Nunes, S. P. & Peinemann, K. V. 2001 *Membrane Technology in the Chemical Industry*. Wiley-VCH, Weinheim, Germany.

Nunes, S. P. & Peinemann, K. V. 2010 *Membrane Technology: Membranes for Water Treatment*, Vol. 4. Wiley VCH, Weinheim, Germany.

Robeson, L. M., Liu, Q., Freeman, B. D. & Paul, D. R. 2015 Comparison of transport properties of rubbery and glassy polymers and the relevance to the upper bound relationship. *Journal of Membrane Science* **476**, 421–431.

Shao, P. & Huang, R. Y. M. 2007 Polymeric membrane pervaporation. *Journal of Membrane Science* **287** (2), 162–179.

So, S., Yao, L. J. & Lodge, T. P. 2015 Permeability of rubbery and glassy membranes of ionic liquid filled polymersome nanoreactors in water. *J. Phys. Chem.* **119**, 15054–15062.

Thomas, S., Wilson, R., Anil Kumar, S. & George, S. C. 2018 *Transport Properties of Polymeric Membranes*. Elsevier, Amsterdam, The Netherlands.

Ulbricht, M. 2006 Advanced functional polymer membranes. *Polymer* **47** (7), 2217–2262.

Wang, Q., Li, N., Bolto, B., Hoang, M. & Xie, Z. 2016 Desalination by pervaporation: a review. *Desalination* **387**, 46–60.

Wijmans, J. G. & Baker, R. W. 1995 The solution-diffusion model: a review. *Journal of Membrane Science* **107** (1–2), 1–21.

Wu, D., Gao, A., Zhao, H. & Feng, X. 2018 Pervaporative desalination of high-salinity water. *Chemical Engineering Research and Design* **136**, 154–164.

Xie, Z., Hoang, M., Duong, T., Ng, D., Dao, B. & Gray, S. 2011 Sol–gel derived poly(vinyl alcohol)/maleic acid/silica hybrid membrane for desalination by pervaporation. *Journal of Membrane Science* **383** (1–2), 96–103.

Xu, J., Hu, Y., Song, L., Wang, Q., Fan, W., Liao, G. & Chen, Z. 2001 Thermal analysis of poly(vinyl alcohol)/graphite oxide intercalated composites. *Polymer Degradation and Stability* **73**, 29–31.

Xue, Y. L., Lau, C. H., Cao, B. & Li, P. 2019 Elucidating the impact of polymer crosslinking and fixed carrier on enhanced water transport during desalination using pervaporation membranes. *Journal of Membrane Science* **575**, 135–146.

Zhang, R., Liang, B., Qu, T., Cao, B. & Li, P. 2017 High-performance sulfosuccinic acid cross-linked PVA composite pervaporation membrane for desalination. *Environ. Technol.* **40** (3), 312–320.

First received 20 December 2018; accepted in revised form 12 March 2019. Available online 28 March 2019